UNIVERSITY *of* York

This is a repository copy of *Energy saving in a 5G separation architecture under different power model assumptions*.

White Rose Research Online URL for this paper:
https://eprints.whiterose.ac.uk/id/eprint/111401/

Version: Accepted Version

Article:

White Rose
university consortium
Universities of Leeds, Sheffield & York

Energy Saving in a 5G Separation Architecture under Different Power Model Assumptions

Abimbola Fisusi*, David Grace, Paul Mitchell

Communications and Signal Processing Research Group, Department of Electronics, University of York, York, YO10 5DD, United Kingdom

ABSTRACT

In this paper, a framework is developed to study the impact of different power model assumptions on energy saving in a 5G separation architecture comprising high power Base Stations (BSs) responsible for coverage, and low power, small cell BSs handling data transmission. Starting with a linear power model function, the achievable energy saving are derived over short timescales by operating small cell BSs in low power states rather than higher power states (termed Low Power State Saving (LPSS) gains) for single and multiple BS scenarios. It is shown how energy saving varies with different power model assumptions over long timescales in accordance with short timescale LPSS. Simulation results show that energy saving in the separation architecture varies across the six power models examined as a function of model-specific significant LPSS state changes. Furthermore, it is shown that if the architecture is based on existing small cell BSs modelled by state-of-the-art (SotA) power models, energy saving will be mainly dependent on sleep state operation. Whereas, if it is based on future BSs modelled by visionary power models, both sleep and idle state operations provide energy saving gains. Moreover, with future BSs, energy saving of up to 42% is achievable when idle state overhead is considered, while a higher saving is possible otherwise.

Key Words: Separation architecture, energy saving, power models, low power state saving, 5G

_____

1. Introduction

Several fifth generation (5G) mobile systems proposals, such as [1] and [2], have identified Energy Efficiency (EE) as an important requirement in 5G systems. This is due to concerns about the economic and environmental consequences of providing 5G services using existing network paradigms mainly focussed on maximizing capacity by increasing transmit power [3]. Already, significant increase in energy consumption of cellular networks has been linked to the large number of smart phones and tablets accessing mobile data and video applications via 3G and 4G networks [4]. Furthermore, increasing demand for mobile data and video traffic has necessitated deployment of more and more Base Stations (BSs) [4, 5]. Further increase in energy consumption is the outcome; this is because BSs account for over 50% of the total power consumption of existing cellular networks [6]. Future 5G systems are expected to support Machine to Machine (M2M) communication which could involve billions of machines [7]. It is also believed that 5G systems will support 1000 times the system capacity of 4G systems [8]. However, providing the desired 1000x capacity by simply scaling transmit powers will result in unacceptable high cost of operation [3] and emission of greenhouse gases beyond acceptable levels [9]. In contrast, the 1000x capacity is required to be provide at energy consumption levels similar to those of current cellular networks [9]. Hence, EE is even more critical for 5G.

In order to address the critical challenge of EE in 5G systems, the concept of separation of the data and control (or signalling) planes has been proposed, with high power macro BSs handling the control functions while low power small cell BSs serve user data only [1, 10]. This approach enables coverage of the service area to be provided by the high power BSs while the capacity needs are met by the low power BSs. As a result, at low traffic loads most of the low power BSs can be switched off without compromising the network coverage requirement. In addition to handling coverage, the macro BSs can be configured to handle low-data rate user requests, while small cell BSs handle high-data rate requests [11, 12]. This type of architecture has been described as a Hyper-cellular network in [13] and referred to as a Separation Architecture in [11]. This architecture can significantly reduce signalling overhead in the small cell layer, optimise the resource utilisation and improve energy efficiency [13]. The energy saving in such an architecture is the focus of this study.

There have been a couple of studies on energy saving in separation architectures. In [12] separation of the data and signalling plane is achieved through small cell, low power data BSs and high power control BSs respectively. The data BSs are activated on demand and switched off when no user is active within their coverage. The signalling BS carries out prediction of the best data BS to serve users based on user location instead of using conventional pilot signal based estimations. The proposed architecture is shown to be 50 times more energy efficient than state of the art (SotA) 2010 systems. Similarly, in [14], the data BSs carry no cell-specific reference (or pilot) signals and are called phantom cells. The phantom cells operate on different frequency bands from the macro layer and hence there is no cross layer interference. EE of the small cell layer is shown to be better in the phantom based approach than a conventional, shared frequency band, heterogeneous network (HetNet).

*Corresponding Author
Email Addresses: aaf504@york.ac.uk (A. Fisusi), david.grace@york.ac.uk (D. Grace), paul.mitchell@york.ac.uk (P. Mitchell)

Whereas [12] and [14] do not seek consistency with existing standards, in [11] a signalling approach suitable for existing wireless standards is considered. As a result, in [11] the small cell data BSs still carry a reduced set of overhead signals including pilot (or reference) signals. However, coverage and low-rate data services are still handled by macro control BSs while data BSs handle high-rate data services. In [15], based on the separation architecture paradigm, a conventional macro BS is replaced with a low power coverage BS (CBS) and several small cell traffic BS (TBS). While the CBS handles coverage, the TBS handles data services. Based on a SotA 2010 model, power consumption is estimated for fixed (TBS always on) and dynamic (TBS on/off) configuration. The separation architecture achieves significant savings (50% or more) over the conventional macro BS approach.

In [16] a separation architecture is proposed for future 5G cellular systems with small cell BSs operated at higher frequencies like 3.5 GHz while the Macro BSs utilise conventional lower frequencies of 2 GHz similar to LTE. Nearly 75% percent energy efficiency gain is achieved since unlike in LTE most small cell BSs can go into deep sleep while macro BSs guarantee coverage. In [17] the joint optimization of density of BSs, number of antennas and spectrum allocation for energy efficiency in a separation architecture based HetNet of macro BSs and small cell BSs is investigated. The combination of small cell BSs and multiple antennas is shown to provide significant energy saving relative to a single antenna macro BSs only system.

The optimal resource partition among signalling and data BSs is studied in [18] while a probabilistic sleep mechanism is designed for the data BS layer of a separation architecture in [19]. In [20] the trade-off between total energy consumption and overall delay for a Data BS of a separation architecture is studied while the ratio of small cell BSs, that can be put to sleep as the traffic load varies, is investigated in [21]. In [22], energy saving is investigated in a separation architecture where the small cells in sleep modes are activated with the help of a macro BS and user association to a small cell is also carried out by the macro BS.

Resource allocation strategies are developed in [23] for a phantom cell based separation architecture to either optimize energy efficiency or optimize spectral efficiency. In [24] on-grid power saving is studied in a separation architecture where small cell BSs can be powered by grid and/or renewable energy sources and are used to offload traffic from macro BSs. In [25] throughput and EE performance is studied in a separation architecture with files cached at the BSs and limited backhaul infrastructure. Furthermore, in [26] sleeping strategies are proposed for a separation architecture in which small cell BSs form co-operative clusters to provide high data services. Also in [27] the effect of BS sleeping on the EE of a small cell BS belonging to separation architecture and the user-perceived delay is studied and optimal energy saving policies are designed under the constraint of mean delay for different wake up schemes. In addition, in [28] an energy saving framework based on feedback information from user equipments is developed for a separation architecture where small cells are user or operator deployed. In [29] a BS sleeping scheme is proposed to put data BSs of a separation architecture into one of two sleeping stages depending on the presence of users in their coverage area.

Furthermore, future evolution of the LTE/LTE-A standard would be able to support separation architectures through the "dual connectivity concept" [30]. Dual connectivity permits user equipment (UE) to be served simultaneously with radio resources from two BSs. Energy saving under the consideration of different backhaul technologies in a separation architecture based on the LTE-A Dual Connectivity is investigated in [31]. In [32] an energy efficient algorithm with consideration of secrecy is proposed for uplink traffic offload in a dual connectivity network with small cell operated in unlicensed band.

Although, the energy savings of separation architectures have been studied under different implementation regimes (as discussed above), the impact of the choice of power model (which depends on the BS generation) on energy saving of a separation architecture has not been studied in the literature to the best of our knowledge. This sort of study is important because it can facilitate an understanding of how energy saving varies with respect to power model assumptions. This knowledge can aid the design of suitable energy efficient resource and topology management strategies or the enhancement of existing strategies.

In this paper, we consider simplified linear power models derived from the initial proposal of the EARTH project [33, 34], which demonstrates that the power consumption of a BS varies linearly with the transmitted power. In addition, we focus on high level aspects of the power models, in this case the variation in the power consumption of a BS in different operating states with different power model assumptions. This variation is due to different BS hardware enhancements expected in the future and suggested in the literature [35-37] and herein. Furthermore, we explore the possibility of the BS power consumption in the idle state approaching the consumption in the sleep state and the power saving when operating small cell BSs in a sleep state and an idle state. Also, we consider a light sleep state only under which few BS components are deactivated and the BS can be quickly reactivated in about 30 µs while the BS enters into a sleep state instantaneously [35].

This is in contrast to the proposal in [38], where detailed BS hardware components' power consumption are considered in the design of a flexible power model suitable for BSs of different types for the period 2010 to 2020. Also in [38], the energy saving potentials of different levels of sleep states is the focus rather than both sleep and idle states and comparison is done for single BS cases rather than in a network of BSs.

Specifically, we examine energy saving in a separation architecture under consideration of six power models and we consider the following questions for the separation architecture:

- Is there significant benefit with regard to energy saving in operating small cell BSs in idle state and sleep state for each power model?
- How do different BS state transitions affect the energy saving for each power model?
- How does the energy saving of these models compare with one another?

We address these questions by developing a framework aimed at evaluating the power saving achievable when BSs are operated in lower power consumption states rather than high power consumption states (termed Low Power State Saving (LPSS)). The framework includes generic equations derived for estimating LPSS over very short timescales for both single and multiple BS scenarios. The short timescale LPSS provide the basis for understanding energy saving over long timescales. Furthermore, a miniature separation architecture model comprising a high power BS and four small cell BSs is also included in the framework to swiftly identify the BS state changes in the small cell layer that contribute significantly to energy savings for each power model. Finally, system level simulation is included to evaluate energy saving and QoS performance of an energy efficient resource management scheme under consideration of the different power models in the full scale architecture.

The remaining section of the paper is organized as follows. In section 2, the system model is presented, while the LPSS framework is discussed in section 3. The simulation results are presented and discussed in section 4. Finally, the paper is concluded in section 5.

2. System Model

2.1. Network Architecture

The access network of the Beyond Next Generation mobile broadband network (BuNGee), which has been modified in this work to include high power control BSs in each zone (referred to as Zone Base Station (ZBS)), is considered. BuNGee is a cost-effective, mobile broadband architecture with the goal of a high capacity density of at least 1Gbps/km^2 studied under the FP7 BuNGee Research project [39]. The BuNGee Architecture is based on a two-tier deployment of access and backhaul network [40]. The access network consists of the BSs that provide resources used to serve user requests while the backhaul network connects the access network to the core network. The BuNGee access network consists of a dense deployment of small cell BSs, referred to as ABSs, in a regular pattern as shown in Fig. 1. The ABSs are low cost, low power, simple, below rooftop BSs. The ZBSs are the control BSs and have been introduced in the access network to facilitate the separation of the control and data plane.

The backhaul network consists of Hub Base Stations (HBSs) and Backhaul Subscriber Stations (BHSSs). The BHSSs are co-located with the ABSs, so at each ABS location there is a complementary BHSS for backhauling Mobile Station (MS) information to a HBS as shown in Fig. 2. The HBSs are high power, wide coverage base stations deployed solely for backhauling. They serve as high capacity hubs for the network through 24-beam, dual-polarized antennas at 3.5GHz [40]. Backhauling is achieved through in-band and millimetre Wave (mmWave) transmissions. The in-band backhauling involves the link between a BHSS and an HBS while the mmWave backhauling involves shorter link distances between BHSSs, due to the shorter range of mmWaves. It is assumed that separate frequency bands are used for the access and backhaul network and interference between the two tiers is completely avoided. Low latency, high capacity and reliable backhaul is provided between the HBSs and BHSSs through the combination of the in-band and mmWave backhauling as demonstrated in [41].

The ABSs are deployed outdoors along the streets in the service area. Each ABS is equipped with two directional antennas which point in opposite directions. One antenna points up the street, the other points down the street. Two ABSs are co-located at the intersection of two streets. The fixed frequency plan [42] specified in the BuNGee project is used here. According to this plan, the two antennas of an ABS operate in different frequency bands. Four directions are considered - North, South, East and West - and an ABS can have North and South pointing antenna beams or East and West pointing antenna beams. In order to mitigate interference, the antennas of adjacent ABSs facing the same direction operate in different frequency bands and two antennas belonging to different ABSs but pointing along the same street also operate in different frequency bands. Four unique frequency bands are assigned to the small cell layer and each frequency band has a bandwidth of 10 MHz. In this work, each frequency band is further divided into 10 unique subchannels and each subchannel on a particular ABS can be assigned to only one MS. Each MS is assigned only one subchannel at a time for uplink transmission.

The MSs are distributed uniformly outdoors in the service area and each MS is equipped with an omnidirectional antenna with a gain of 0 dBi. The service area is divided into nine square zones as shown in Fig. 1 and ABSs can be associated with up to a maximum of four zones. ABSs can only communicate directly with their adjacent neighbours while they can communicate with the ZBSs through backhaul links. The ZBSs share a 10 MHz frequency band that is out of band to the ABS bands.

In line with the separation architecture paradigm, the ZBSs deployed in the zones are always on to provide universal coverage for the MSs while the ABSs, which can be switched on and off, and provide data services. Hence, an MS is always connected to the ZBS in its current zone while it can utilize resources on any ABS in the zone depending on the channel quality and resource management scheme adopted. This is similar to the functionality separation in [11] which has been shown to result in up to 50% reduction in overhead signal transmission of the small cell BSs relative to 4G systems utilizing cell-specific reference signal (CRS) [43]. Therefore, a reduction of 50% is adopted in this study.
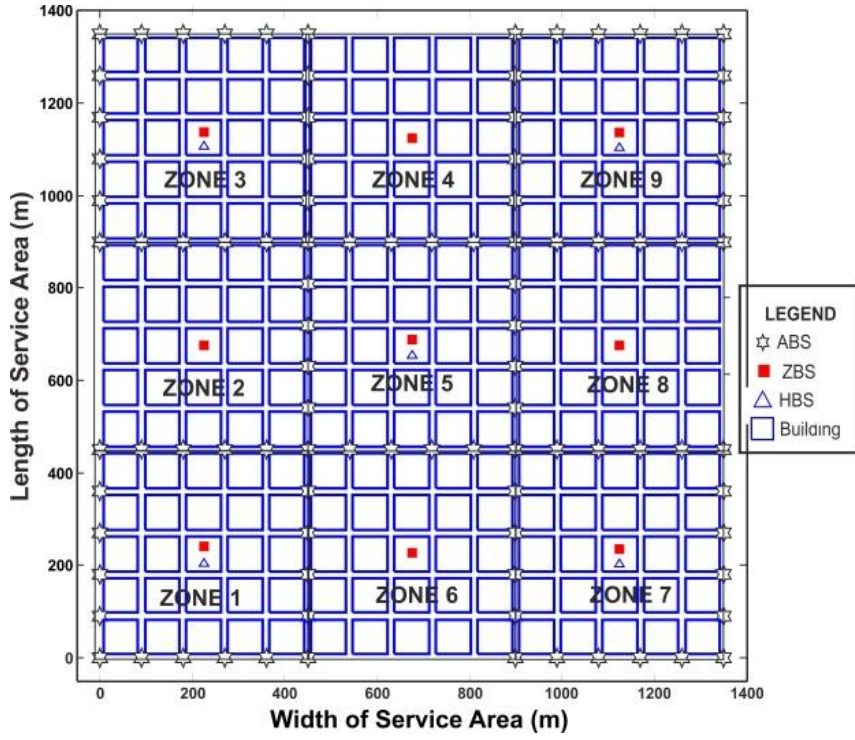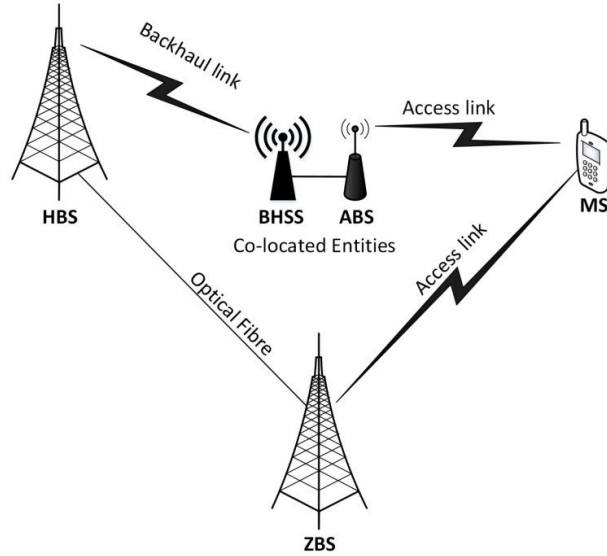
Fig. 1. BuNGee Topology

Fig. 2. BuNGee Access and Backhaul

As shown in Fig. 2, each ZBS is connected to a nearby HBS through optical fibre and information exchange is possible with low delay between a ZBS and an ABS through the backhaul links between a HBS and a BHSS. mmWave links between BHSSs may also be utilized for diversity in case of failure of the direct link between HBS and a particular BHSS. Whenever an MS has to be served in the DL or UL, the serving ZBS requests the ABSs in its zone to send channel quality measurement in respect of the concerned MS. The channel quality measurement used here is the signal to noise plus interference ratio (SINR). The ZBS will then determine the ABS to serve the MS depending on the objective of the resource management scheme adopted. This co-ordination procedure between the ZBSs, ABSs and MSs before data transmission is similar to the one in [13] and it is illustrated in Fig. 3 for the UL.
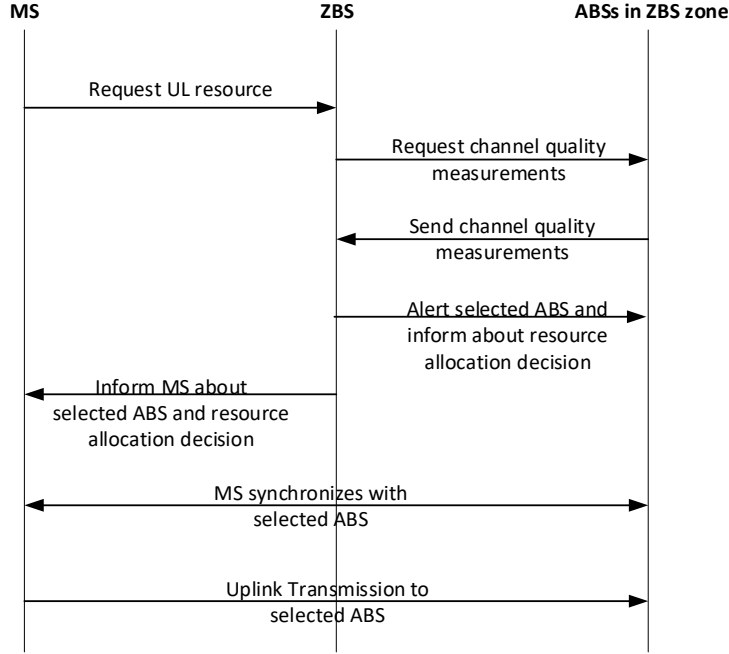
Fig. 3. Co-ordination Procedure for UL Data Transmission

The channel between an ABS and a MS is modelled using the WINNER II B1 propagation model for Urban Micro-cells [44] since the ABSs and MSs are deployed outdoors. The transmission rate per bandwidth, R, over the channel is determined from the Truncated Shannon Bound (TSB) [45] as follows:

$$R = \begin{cases} 0 \,; & \text{for } SINR < SINR_{min} \\ \alpha \log_2(1 + SINR) \,; & \text{for } SINR_{min} < SINR < SINR_{max} \\ R_{\max} \,; & \text{for } SINR > SINR_{max} \end{cases} \quad (1)$$

α is the attenuation factor, $SINR_{min}$ is the minimum SINR required for reception, $SINR_{max}$ is the SINR at which the maximum throughput, R_{max} can be achieved. The parameters of the BuNGee-specific TSB [42] are $\alpha = 0.65$, $SINR_{min} = 1.8$dB, $SINR_{max} = 21$dB and $R_{max} = 4.5$bps/Hz.

2.2. Power Consumption and Energy Saving

The power consumption of the access network is estimated to be 80% of the entire wireless network consumption and the base stations are mainly responsible for this huge share of the access network [46]. Therefore, the energy saving at the BSs is the focus in this work. In particular, we consider the energy savings that can be achieved in the access network by switching some of the ABSs into low power consumption states when uplink data transmissions from MSs are being served. The power consumption of the backhaul network including the HBSs and BHSSs are not considered but the backhaul network have been explained earlier to show how information exchanges between ZBSs and ABSs in the access network can be implemented practically.

In existing wireless systems, unlike in macro BSs where the load dependent power amplifier (PA)

consumption is dominant (55-60%), for low power BSs (i.e. micro, pico, and femto BSs) the PA share of the power consumption is much smaller (less than 30%) in currently deployed systems [34]. Hence, power consumption of micro BSs are much less load dependent than macro BSs while power consumption of pico and femto BSs hardly scale with load [33]. As a result, the full load downlink power consumption of small cell BSs is of similar order of magnitude as the uplink and no load conditions in existing systems. Hence, it is important to consider the energy savings at BSs in the uplink for a network with an ultra-dense deployment of small cells.

3. Framework for LPSS Evaluation

Generally, a BS can operate in active, idle, or sleep states. In the active state, it receives and/or transmits data, whereas in the idle state it is powered on but waiting to serve user requests. When traffic levels permit, a BS can be operated in the sleep state where it consumes lower power than in the active or idle states, but cannot serve user requests. A BS can achieve some power saving when it operates in a low power state rather than a higher one. The power saving due to BSs operating in low power states rather than higher states (termed Low Power State Saving (LPSS)) under different power model assumptions is examined for uplink transmission.

As mentioned earlier, we consider a light sleep state with a few BS hardware components deactivated so that the BS can be reactivated in about 30 µs while it enters into the sleep state instantaneous [35]. Thus, with regard to flow level modelling considered in this paper, the time taken to switch from one state to another is assumed to be negligible

since file transmissions take significantly longer time compared to the reactivation time of about 30 μs.

3.1. Power Models

Power models are usually required to estimate the total power consumption of a BS. These models usually comprise a static part and a dynamic part. The static part is independent of the traffic load and output transmission power. It instead includes losses in the power supply, signal processing, and cooling systems [47]. On the other hand, the dynamic part is dependent on the traffic load supported by the BS and thus a function of the output transmission power. The power consumption of any type of BS can be approximated by a linear function [33, 34] as follows:

$$P_{in} = \begin{cases} N_{TRX}(P_0 + \Delta p. P_{out}), & 0 < P_{out} \leq P_{max} \\ N_{TRX}. P_{sleep}, & P_{out} = 0 \end{cases} \quad (2)$$

P_{in} is the BS total power consumption, P_{out} is the output transmission power, P_{max} is the maximum transmission power, P_0 is the no load power consumption measured at the lowest possible non-zero output power, N_{TRX} is the number of transceiver chains, while Δp is the slope of the load dependent dynamic consumption part. P_{sleep} is the power consumption when the BS is switched to sleep state. The sleep state consumption, P_{sleep}, is lower than the no load consumption, P_0, because it is assumed that in the sleep state, some BS components can be deactivated to further reduce power consumption [48].

Even in the idle state, when no user data is transmitted by a BS, between 10% and 20% of the maximum transmission power is used to transmit reference and control signals (which constitutes overhead) in state-of-the-art (SotA) cellular systems (e.g. LTE) [49]. Hence, the instantaneous output transmission power, P_{out}, is a combination of the power needed for signalling and power for user data. According to [50] for SotA cellular systems, the instantaneous output transmission power is given by:

$$P_{out} = (1 - p_{OH})P_{max} \rho_b + p_{OH}P_{max} k \quad (3)$$

p_{OH} is the fraction of the transmit power required for fixed overhead signals ($0 \leq p_{OH} < 1$), ρ_b is the fraction of the total bandwidth used for data transmission, and k is a weighting factor that indicates the level of overhead transmitted depending on the state of the BS ($0 \leq k \leq 1$). The value of k for different states are as follows [50]:

$$k = \begin{cases} 0 & sleep \\ 0.5 & idle \\ 1 & active \end{cases} \quad (4)$$

In the sleep state, both overheads and user data are not transmitted, partial overheads are transmitted in the idle state, while the complete set of overheads is transmitted in the active state. p_{OH} is assumed to be 0.2 herein, since as

stated earlier, up to 20% of the maximum transmission power may be used to transmit overheads [49].

For uplink transmission, BS transmit power is expended on overhead only since no user data is transmitted by the BS. Hence, $\rho_b = 0$ and the output transmit power, P_{out}, is as follows for the uplink case only:

$$P_{out} = p_{OH}P_{max} k \quad (5)$$

As stated earlier, up to 50% reduction in overhead signal transmission relative to 4G systems utilizing CRS is possible at the small cell BSs through the separation architecture [43]. Hence, from (4) overhead weighting factor under the separation architecture, k_s, equivalent to 50% overhead reduction is adopted herein for each BS state as follows:

$$k_s = \begin{cases} 0 & sleep \\ 0.25 & idle \\ 0.5 & active \end{cases} \quad (6)$$

While the energy consumption of the small cell BSs can vary with the operating state, the energy consumption of the ZBSs is assumed constant since the ZBSs are always on and can be considered to always be in the idle state since the case of data transmission by the small cell BSs alone is considered herein.

The linear function in (2) can be expressed in terms of static and dynamic parts and with the incorporation of the three possible BS states as follows:

$$P_{in} = P_{st} + \Delta p. P_{dy}, \quad 0 \leq P_{out} \leq P_{max} \quad (7)$$

$$P_{st} = \begin{cases} N_{TRX}. P_0, & Other\ states \\ N_{TRX}. P_{sleep}, & Sleep\ states \end{cases} \quad (8)$$

$$P_{dy} = \begin{cases} N_{TRX}. P_{out}, & Other\ states \\ 0, & Sleep\ state \end{cases} \quad (9)$$

P_{st} is considered to be the static power consumption. This is because P_0 is a parameter that represents BS power consumption at zero output but which is usually measured at 1% of the maximum output transmit power [51]; P_{sleep} also measures power consumption at zero output but with some BS components deactivated. P_{dy} is considered as the dynamic part since the output transmit power varies with the load. The variation could be due to reduction in occupied subcarriers and/or subframes [33].

Each ABS is classified as a 2x2.5W Microcell BS with a maximum transmission power of 5W (i.e. $N_{TRX} = 2$). Since power model parameters for the 2x2.5W ABS are not available explicitly in the literature they have been derived. The maximum power consumption of any generic SotA 2010 BSs (i.e. Macro, Micro, Pico or Femto BS) can be obtained from the linear function specified in [15]. According to [15], the power consumption of any type of SotA 2010 BS at full load, $P_{in}^{F\_Load}$, is a linear function of the full load (or maximum) transmission power, P_{max}, as follows:

$$P_{in}^{F\_Load} = a.P_{max} + b \qquad (10)$$

$P_{in}^{F\_Load}$ and P_{max} are dBm power values, while a and b are constants: $a = 0.618$ and $b = 26.1$. From (10) the maximum power consumption of each 2x2.5W ABS is 102.6W. Other relevant power model parameters of the ABSs can be obtained from (2).

Six power models ranging from a state-of-art 2010 (SotA 2010) model to a future model are considered. Four of the models – SotA 2010, Improved DTX, Market 2014 and Future Models – were previously considered in [37] for a single macrocell scenario. The Han model proposed in [52] and Beyond 2020 model (proposed in this study) complete the set of power models. The ABS specific linear model parameters for the different models are provided in Table 1 for a single transceiver chain.

Table 1

Linear Model Parameters for Different Power Models

Model	P_0 (W)	Δp	P_{sleep} (W)
SotA 2010	44.8	2.6	31.4
Improved DTX	44.8	2.6	2.7
Market 2014	17.9	2.6	2.7
Beyond 2020	1.2	7	1
Han	2.78	4.44	0.14
Future	0.1	7	0.1

The SotA 2010 model is based on the linear power modelling of SotA BS types in 2010 proposed in [34]. The SotA 2010 model is specified for a 2x6.3W microcell in [34]. The parameters for the 2x2.5W ABS considered herein are obtained using (2) as follows. Assuming the same slope, $\Delta p = 2.6$, as in [34] and with the maximum power consumption and maximum transmission power (102.6W and 2.5W per transceiver chain respectively) already known, the no load consumption, P_0, can be determined from (2). The sleep state consumption, P_{sleep}, is obtained from the ratio between the sleep and no load consumption in [34].

The improved DTX model proposed in [35] assumes that significant power consumption reduction can be achieved through cell DTX, which is a procedure that switches the BS to sleep state. This is because sleep state consumption is only approximately 6% of the no load consumption. However, the no load consumption is unchanged since enhancement of BS hardware is not considered in this model. The Market 2014 model (so called in [37]) suggested in [36] assumes that in addition to the sleep mode capability, BSs are designed with more power efficient components in the future. Hence, a substantial reduction in no load consumption (approximately 40%) is assumed in addition to the sleep mode saving.

A beyond 2020 model is also proposed to reflect the expected design of BSs to have nearly perfect load dependency and very low sleep and no load power consumption. Hence, a sleep mode consumption that is much lower than the 2014 status is assumed. In addition, rather than a 100 percent increase in power from the sleep to no load consumption assumed for a 2020 small cell model in [53], a much lower increase of 20% is assumed in this case. This model is used to explore the impact of idle state consumption (a function of the no load consumption) approaching the sleep state consumption. The Han model, proposed in [52], assumes a relatively low no load power consumption and nearly zero sleep mode consumption. In addition, it accounts for power consumed in reactivating a BS in sleep state. However, the contribution of reactivation energy has been observed to be trivial and it is not considered in the linear adaptation of this model. The extra power cost incurred by signalling is not accounted for in all states and ABSs transmit at maximum power when active under this model.

Finally, the Future model proposed in [37] provides a theoretical limit for power consumption. This model results in a near perfect load-dependent power consumption; also, the no load consumption is exactly the same as the sleep state consumption. It is assumed here that no extra power cost is incurred for overhead ($k = 0$) in the idle state. This is possible with overhead transmission completely disabled in the idle state. However, overhead power is included in the active state (uplink/downlink). Hence, power is mainly utilized when users are being served.

3.2. Short Timescale LPSS in Single BS Scenario

An ABS can be in any of the three possible states at a given time and may make the transition to a different state after a period of time (as shown in Fig. 4). In the same vein, an ABS may operate in a particular state under a certain resource management scheme but operate in a different state under another scheme for a similar observation period and system settings. When the ABS is monitored over a very short timescale of the order of magnitude of the time between user arrivals or departures (few milliseconds to seconds), it is possible to observe single state changes. Over longer timescales (a couple of minutes or hours), the ABS may undergo several state changes. We first focus on the short timescale and develop the LPSS concept. Subsequently, LPSS over the long timescale is considered.

If an ABS changes state under the control of a resource management scheme from an initial state in which its power consumption is P_1 to a new state where it consumes P_2 and remains in this new state for a time period, t; some power saving (LPSS) will be achieved as a result of this state change for the considered period, t, if $P_1 > P_2$. Similarly, if an ABS is monitored over a fixed period of time and fixed system setting (e.g. fixed traffic load and distribution) under two different resource management schemes, one scheme can achieve power saving relative to the other if the ABS effectively operates in different states under the different schemes. The equations derived subsequently are applicable to both the state change and the state difference cases and both are used interchangeable.
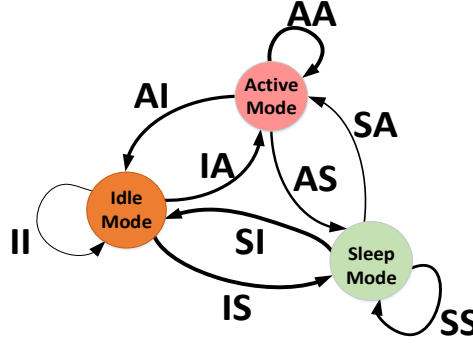
Fig. 4. BS Possible State Changes

Whenever there is a state change, there is a potential increase or decrease in power consumption relative to the initial state. However, only the active to idle (AI), active to sleep (AS) and idle to sleep (IS) state changes lead to power saving. From (7), we can obtain a generic expression for the LPSS due to any of the state changes above. If the BS was initially in a state 1 and changes to a new state 2, the LPSS, P_{12}, can be expressed as follows:

$$P_{12} = P_{st,1} - P_{st,2} + \Delta p(P_{dy,1} - P_{dy,2}) \quad (11)$$

$P_{st,1}$, and $P_{st,2}$ are the static power consumption in state 1 and state 2 respectively, while $P_{dy,1}$ and $P_{dy,2}$ are the dynamic power consumption in state 1 and state 2 respectively. Δp is the slope of the dynamic part. The LPSS gain, $P_{G,12}$, which expresses the LPSS, P_{12}, as a ratio of the power consumption in the initial state, P_1, can be defined as follows:

$$P_{G,12} = \frac{P_{12}}{P_1} = \frac{P_{st,1} - P_{st,2} + \Delta p(P_{dy,1} - P_{dy,2})}{P_{st,1} + \Delta p.P_{dy,1}} \quad (12)$$

The LPSS gains for different state changes under different power model assumptions for a single BS are shown in Fig. 5. The uplink is considered in this study; thus, the active state represents the periods an ABS is receiving data transmission from MSs. It can be observed from Fig. 5 that the significant state changes and the potential for power saving varies from model to model. The SotA 2010 model shows the lowest potential for power saving because it has comparatively high no load consumption and sleep mode consumption, resulting in a lower range of power saving. Other models show better potential for power saving because of significantly lower sleep state consumption and in some cases low static consumption. The SotA 2010, Improved DTX and Market 2014 show almost no benefit for operating the ABS in an idle state. On the other hand, the remaining models, show appreciable power savings when an ABS is operated in an idle state instead of an active state. It is important to note that power saving is still possible for the idle state to the sleep state transition even when the no load consumption,

P_0, is almost equal to sleep mode consumption, P_{sleep}, because of the extra power incurred in the idle state for overhead signals in non-ideal models as in the case of Beyond 2020 model. The Future model, which is an ideal model, alone does not benefit from switching idle BS to sleep state since consumption is the same in both states.

3.3. Short Timescale LPSS in Multiple BS Scenarios

The LPSS concept is also extended to multiple BS scenarios comprising several BSs. This is typical of the small cell layer of the separation architecture. In this case, the LPSS gains are expressed in terms of the relative importance of the different state changes on a global scale (i.e. multiple state changes and multiple BSs). The equations are derived based on state differences and assumption of different resource management schemes.

It is assumed that the first scheme is a baseline resource management scheme that requires all ABSs to always be on (i.e. either in active or idle state). This is similar to conventional always-on resource management schemes with the goal of spectral efficiency rather than energy efficiency. The second (test) scheme is an energy efficiency driven scheme and can switch off (or switch to the sleep state) BSs under favourable conditions. With the baseline scheme as the reference scheme, the LPSS gains can be evaluated for the test scheme.

The total power consumption of the baseline and test schemes are $P_{baseline}$ and P_{test} respectively and expressed as follows:

$$P_{baseline} = \sum_{j=1}^{n}(P_{st,b,j} + \Delta p.P_{dy,b,j}) \quad (13)$$

$$P_{test} = \sum_{j=1}^{n}(P_{st,t,j} + \Delta p.P_{dy,t,j}) \quad (14)$$

n refers to the total number of BS, b represents a BS state under consideration of the baseline scheme while t similarly represents a BS state under consideration of the test scheme. Therefore, $P_{st,b,j}$ and $P_{dy,b,j}$ are the static and dynamic power consumption of the jth BS in state b with consideration of the baseline scheme. Similarly, $P_{st,t,j}$ and $P_{dy,t,j}$ are the static and dynamic power consumption of the jth BS in state t with consideration of the test scheme.
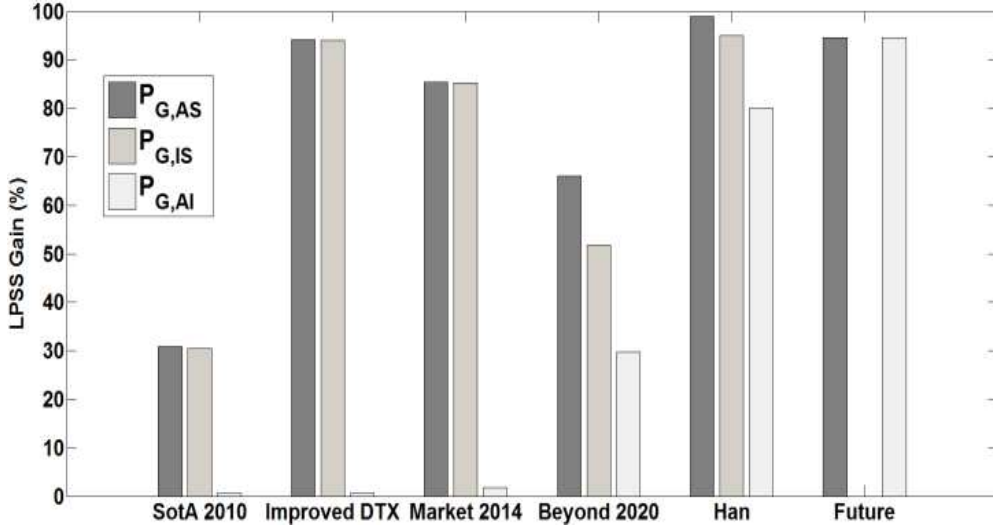
Fig.5. LPSS Gains for Single BS

Therefore, following from (13) and (14), the total power saving of the test scheme with respect to the baseline scheme, P_{saving} is as follows:

$$P_{saving} = P_{baseline} - P_{test}$$
$$= \sum_{j=1}^{n}(P_{st,b,j} + \Delta p. P_{dy,b,j}) - \sum_{j=1}^{n}(P_{st,t,j} + \Delta p. P_{dy,t,j}) \quad (15)$$

Two types of LPSS gain is defined for the multiple BS case: absolute and comparative. On one hand, the absolute LPSS gain, $P_{A,bt}$, measures the actual saving due to a particular state difference between the test and baseline scheme for the period of observation with respect to the baseline power consumption. On the other hand, the comparative LPSS gain, $P_{C,bt}$, measures the saving of a particular state difference with respect to the total saving. Thus, the comparative LPSS gain shows explicitly the share of a particular state difference combination in the total saving whereas the absolute LPSS gain just shows its actual value. If P_{bt} is a LPSS of a single BS (*kth* BS) as defined in (11), then the absolute LPSS gain, $P_{A,bt}$, and comparative LPSS gain, $P_{C,bt}$, can be expressed as follows:

$$P_{bt} = P_{st,b,k} - P_{st,t,k} + \Delta p(P_{dy,b,k} - P_{dy,t,k}) \quad (16)$$

$$P_{C,bt} = \frac{P_{bt}}{P_{saving}} = \frac{P_{st,b,k}-P_{st,t,k}+\Delta p(P_{dy,b,k}-P_{dy,t,k})}{\sum_{j=1}^{n}(P_{st,b,j}+\Delta p.P_{dy,b,j})-\sum_{j=1}^{n}(P_{st,t,j}+\Delta p.P_{dy,t,j})} \quad (17)$$

$$P_{A,bt} = \frac{P_{bt}}{P_{baseline}} = \frac{P_{st,b,k}-P_{st,t,k}+\Delta p(P_{dy,b,k}-P_{dy,t,k})}{\sum_{j=1}^{n}(P_{st,b,j}+\Delta p.P_{dy,b,j})} \quad (18)$$

Hence, $P_{A,bt} = P_{C,bt} \times \frac{P_{saving}}{P_{baseline}} = P_{C,bt} \times P_{gain} \quad (19)$

Where P_{gain} is the overall power saving gain of the test scheme relative to the baseline. Subsequently, comparative LPSS gain is evaluated over a snapshot of the BuNGee network using two resource management schemes previously proposed for the BuNGee Architecture as baseline and test schemes. It is important to note that MS arrivals are modelled by flow level dynamics, which constitutes a random arrival of MSs into the network each with file transfer requests and departures from the network when files have been successfully transferred [38]. We consider the case where MSs send one file at a time and are assigned one subchannel for this purpose.

3.4. Resource Management Schemes

In some previous BuNGee evaluations [42, 52] the resource management strategy associates MSs with the closest ABSs that can offer them the highest uplink SINR. We refer to this scheme as the highest SINR scheme and use it as the baseline scheme. Under the control of this baseline scheme, the ABSs are never switched off (i.e. transition to a sleep state is not permitted).

The test scheme is a combination of a resource management scheme and a topology management scheme for multiuser resource assignment and ABS activation or deactivation respectively. The test resource management scheme is the Interference Aware Clustering Capability Rating (IACCR) scheme, which we proposed previously for the BuNGee architecture without plane separation [54]. The IACCR is an energy efficient centric scheme that also mitigates interference as well [54], while the topology management scheme is an enhancement of the one applied in our previous studies on BuNGee [54, 55].

3.5. Highest SINR Scheme

This scheme's objective is to associate MSs with the closest and first choice ABS in terms of the magnitude of the SINR (highest SINR) in order to maximize throughput and system capacity density. In the separation architecture considered herein, the decision of the ABS and the radio resources an MS can utilize is made by the ZBS which acts as the Control BS. When an MS requires uplink resources, it makes the request to the ZBS and the ZBS in turn

requests for the uplink SINR of the subchannels from the ABSs for the specific MS. However, only ABSs with uplink SINR subchannels higher than the call admission SINR threshold need respond. The ZBS will then instruct the MS to connect to the ABS with the highest SINR subchannel.

3.6. Interference Aware Clustering Capability Rating (IA-CCR) Scheme

Interference Aware Clustering Capability Rating (IA-CCR), proposed in [54], is an enhancement of the Normalized Clustering Capability Rating (NCCR), an energy efficient resource management scheme proposed in [55] for the BuNGee Architecture. NCCR is based on the principle of concentrating or clustering users around as few as possible ABSs, thus permitting a large number of ABSs to be switched off. The scheme prefers more central ABSs over those closer to the edge of the service area to serve MSs. This is because of the potential of the more central ABSs to cluster more users based on their location in the service area. The choice of ABS is based specifically on the computation of a clustering capability rating (CCR) value. The CCR value is a linear combination of two ABS location parameters and one ABS load parameter and it is evaluated as follows:

$$CCR = aZ_a + bL_w + cL_r \qquad (20)$$

The location parameters are the zone association weight, Z_a, and location weight, L_w. The zone association weight, Z_a, is the number of zones an ABS is associated with normalized by the maximum possible zone association (which is 4). The location weight, L_w, is the reciprocal of the normalized distance of an ABS to the centre of its zone. The ABS distance is normalized by the distance of the most central ABS to centre of the zone. The load parameter is referred to as the loading ratio, L_r, and it is the ratio of the instantaneous traffic load on an ABS to the maximum traffic load it can support. These parameters have values between 0 and 1 due to the normalization in all cases. a, b, and c are constants, and $a = 100$, $b = 10$, and $c = 1$. These constants are used to achieve hierarchical scaling among the ABS parameters. The final NCCR value is obtained from the normalization of the CCR value by the maximum possible CCR value as follows:

$$NCCR = \frac{CCR}{CCR_{max}} \;;\; CCR_{max} = 111 \qquad (21)$$

An MS is served by an ABS with the highest NCCR value that meets the call admission SINR threshold.

At low traffic loads, the NCCR scheme can significantly reduce the number of active ABSs and provide opportunity for energy savings through deactivation of idle ABSs [55]. However, at medium and high traffic loads, it causes high interference in the network which in turn leads to both poor quality of service and low energy efficiency [55]. In [54], it is shown that the choice of ABS determines

the level of inter-cell interference among the small cell ABSs in the network. While, the highest SINR scheme which associates an MS with the closest and first choice ABS in terms of SINR results in low interference, the NCCR scheme permits MS association with any choice of ABS, which includes distant and higher order choices and thus results in very high interference.

The IACCR scheme mitigates the interference associated with the NCCR scheme whilst still achieving a good degree of clustering and energy saving. This is achieved by first applying a restriction policy that limits the ABS choice range for an MS before the final choice of ABS is made based on the NCCR value of the permitted choices. In this study, the choice of ABS to serve an MS is made by the ZBSs rather than the MS itself like in [54]. The IACCR scheme is implemented as follows: let L_i and L_{max} represent the current traffic load and maximum possible traffic load of an ABS i respectively; thus, the normalized traffic load, x_i on ABS i at any instant can be expressed as:

$$x_i = \frac{L_i}{L_{max}} \qquad (22)$$

Let $X = [x_i]$ represent the vector of the normalized traffic load of all ABSs in the zone, while $S = [s_i]$ represent the vector of the highest uplink channel SINR achieved at each of the ABSs. Let $C = [c_i]$ represent the NCCR vector for the ABSs while s_{th} represent call admission SINR threshold. Given an nth choice restriction policy specified in the service area, which implies MSs are permitted to connect to the nth choice ABS or lower order (but better) choices, the final choice of ABS is determined as follows:

1. All elements of X, S and C are set to zero initially.
2. When MS requests for uplink resource, ZBS requests channel quality measurement from ABSs in its zone.
3. Each ABS verifies the condition: $s_i \geq s_{th}$ and sends s_i to ZBS only if the condition is satisfied.
4. ZBS updates S with all received s_i, C with c_i for each ABS that responds, and then arranges the set of ABSs in descending order of SINR (s_i). However, if no ABS responds, the MS is blocked.
5. Assuming the total number of ABSs in the set is m, a ZBS will instruct the MS to connect to an ABS with highest c_i value among the set of ABS, if $m \leq n$. However, if $m > n$ ZBS selects the highest ranking n ABSs based on s_i, and instructs the MS to connect to the ABS with highest c_i value in the high ranking ABS subset.
6. ZBS updates X to account for the increase in traffic load and resets all the elements of S and C in preparation for a new MS request. Step 1 is not repeated after the first MS request.

The topology management scheme is used to activate and deactivate ABSs in sleep and idle states respectively. The rules governing the operation of the topology management scheme are explained next.

3.7.   Topology Management Scheme

The topology management scheme proposed in [55] is enhanced and applied here. We improve on the topology management by using variable duration rather than the fixed duration irrespective of traffic load used in [55] for the expended time before switching off an idle ABS and for monitoring blocking in each zone. The rules for switching ABSs off and on under the enhanced topology management scheme are as follows:

ABS switch off rules:
1. ABS traffic load capacity = 0 consistently for a period of T_{off} and
2. All ABS neighbour load capacities $< C_{off}$
ABS switch on rules:
1. ABS neighbour load capacity$\geq C_{on}$ or
2. Blocking in zone $= N_b$ in a period, $t \leq T_{on}$

$C_{off} = 50\%$, and $C_{on} = 90\%$ of maximum traffic load capacity of ABSs, C_{max}. These values are chosen to allow prompt switching off at a moderately low neighbour load level and sufficient waiting period before switching on ABSs at significantly high neighbour load level. An idle ABS is switched off (ABS switch off rule 1) if no MS is assigned to it within the time required for at least one neighbour ABS to reach the switch off load threshold, C_{off}, based on the average zonal MS inter-arrival time, T_{int}, in the zone. Thus the waiting time, T_{off}, before switching off is given by:

$$T_{off} = C_{off} . C_{max} . T_{int} \tag{23}$$

The blocking probability target of 5% is assumed. Specifically, the blocking is counted and ABSs with the highest CCR are switched on if the blocking exceeds a total of 5 in a duration (based on the average zonal MS inter-arrival time, T_{int}) required to have 100 MS requests or less (ABS switch on rule 2). Thus, $N_b = 5$ and the blocking duration, T_{on} is given by:

$$T_{on} = 99 . T_{int} \tag{24}$$

This blocking duration measures the expected time on average between the 1st MS request and the 100th MS request.

3.8.   Comparative LPSS Gain in BuNGee Snapshot

We consider a multiple BS scenario comprising four ABSs of the BuNGee Architecture and assume a short timescale exist that contains all three power saving state differences (i.e. AI, AS, IS) of the baseline scheme relative to the test scheme as shown in Fig. 6. Only one case of each power saving state difference is observed across all ABSs and each ABS is associated with only the indicated state difference during this short timescale. The combinations in Fig. 6 are considered in order to compare all three power saving state differences under an equal weighting regime of one occurrence per state difference. This is used to obtain evenly weighted comparative LPSS gain for all the power models and to show the significance of each state difference to power saving on a more global level than the single BS case. Thus, identifying the BS state differences that are significant with respect to energy saving. Absolute LPSS gains can be obtained from comparative gains using (19).

We illustrate the state differences of Fig. 6 in a real service area with a snapshot of BuNGee streets with MSs, ABSs and ZBSs in a zone as shown in Fig. 7. Only the frequency band of antennas pointing in the zone is shown for the ABSs and the energy calculation is done for the single transceiver chain of each ABS serving the zone. Thus, each ABS is modelled as a single transceiver ABS.

We assume that the six MSs are the only active users that arrived with uplink requests and allocated resources prior to the short timescale considered. In addition, it is assumed that no MS departure occurs during the short timescale. As mentioned earlier, each MS is assigned one subchannel out of 10 subchannels configured on each ABS antenna, thus the level of ongoing traffic is low when compared to a capacity of 40 MSs that can be supported theoretically by the four ABS antennas actively serving the zone.

Since the traffic level is low, interference will be low as well and a single ABS can serve all six MSs. However, based on the baseline scheme, the highest SINR scheme, the ZBS assigns MSs to the closest ABSs that can give the highest SINR. Hence, it is expected that ABS 1 will serve MS 3 and MS 4; ABS 3 will serve MS 1; while, ABS 4 will serve MS 2, MS 5 and MS 6. Therefore, during the short timescale considered, ABS 1, ABS 3 and ABS 4 will be in an active state while ABS 2 will be in idle state since ABS deactivation (sleep state) is not supported under the baseline scheme. On the other hand, the test resource management scheme (IACCR) is based on the concept of clustering MSs around few ABSs as long as the ABSs are permitted choices. Assuming that ZBSs permit MSs to use resources from up to the fourth choice ABS, then all the MSs can be served by ABS 4 or ABS 1 which are the most central ABSs. MSs are clustered using ABS 4 as an example in this scenario. Since, ABS4 will be serving six MSs with greater than 50% of its resources (60% precisely), this will prevent the switching off its neighbour, ABS 3, according to the topology management ABS switch off rule 2 . However, ABS 1 and ABS 2 can be switched off (sleep state) since the switching off rules are satisfied for both of them. Thus for the test scheme, ABS 1 and ABS 2 will be in sleep state, ABS 3 in idle state and ABS 4 in active state. Therefore, comparing the baseline and test schemes, we have the three power saving state differences in three ABSs and no state difference in one ABS as shown in Fig. 6. From (17) and (19), the comparative LPSS and overall power saving gain, P_{gain}, can be calculated under consideration of the different power models for this scenario. These are shown in Fig. 8.
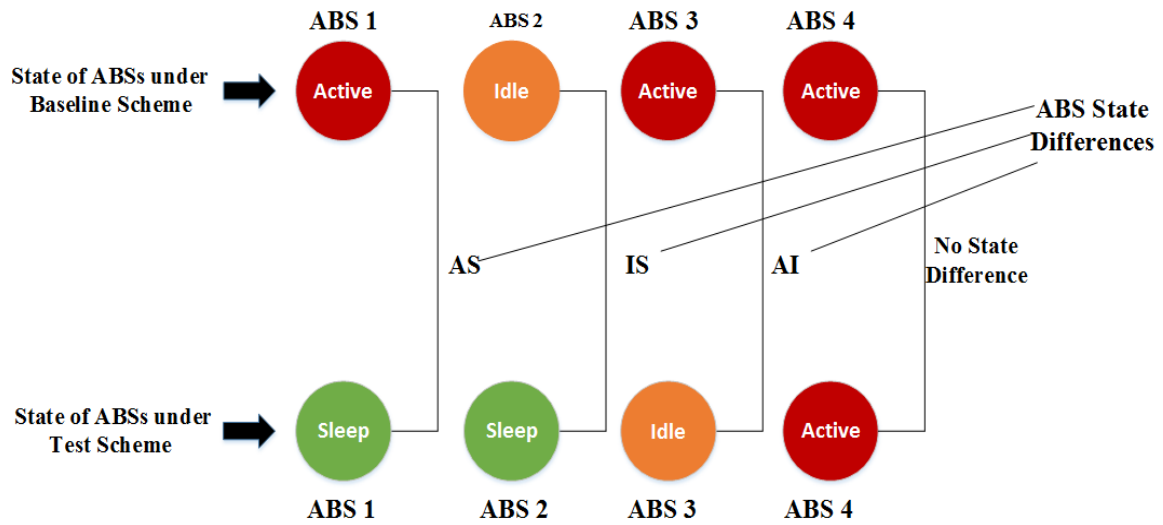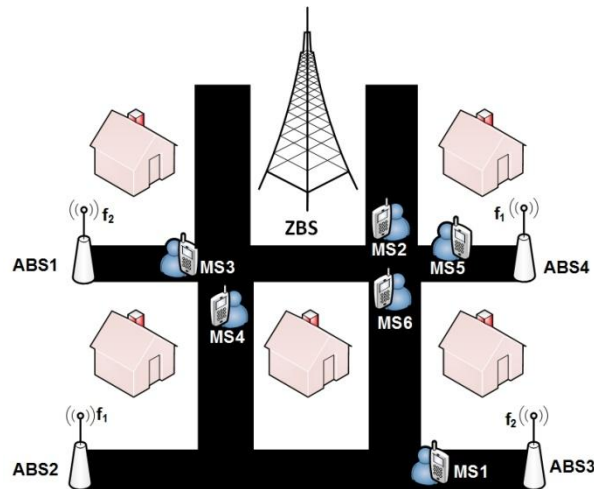
Fig. 6. Multiple BS State Change Saving Concept

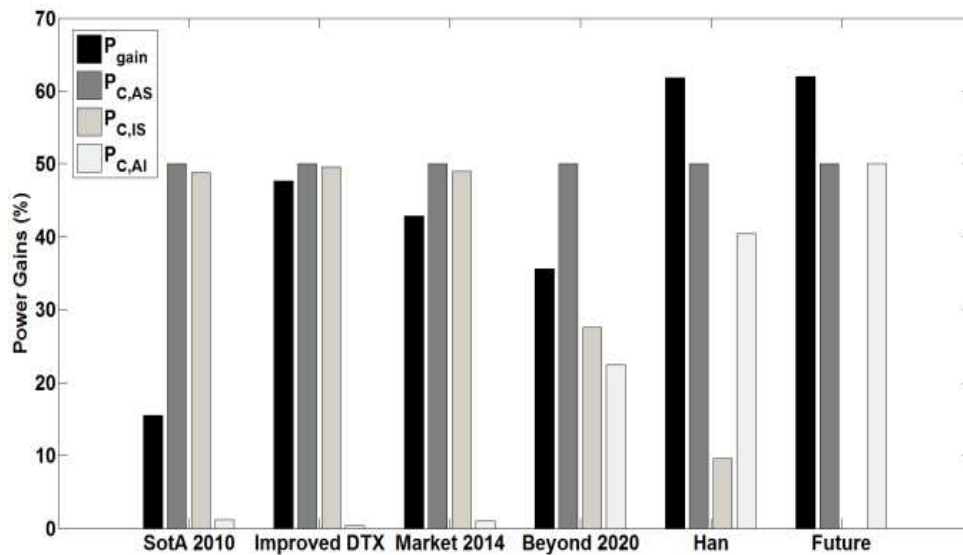**Fig. 7.** BuNGee Snapshot of Streets with ABSs and MSs

Fig.8. Power Saving Gain and Comparative LPSS for BuNGee Snapshot

It is observed in Fig. 8 for the overall power saving gain, P_{gain}, that the SotA 2010 shows the lowest potential for power saving just like in the single BS case. Furthermore, since the comparative LPSS gains are evenly weighted, only the state differences that end in sleep states (i.e AS and IS) are significant for energy saving with regard to SotA 2010, Improved DTX and Market 2014 models. On the other hand, all state differences contribute to energy savings to varying degrees under Beyond 2020 and Han models. However, AS is the most significant in both cases. For the Future model, IS is of no benefit to energy saving while AS and AI are equally significant.

3.9. Long Timescale LPSS

In the previous sections, we focussed on short timescale LPSS with only one power saving state difference occurring per ABS. However, when an ABS is observed over a long period under flow level dynamics, apart from state differences associated with power saving, state differences associated with power losses can also be observed and also no state differences at all. Assuming that an ABS is observed over a long timescale that is divided into very short timescales, then energy saving will be achieved if and only if the total saving from power saving state differences exceeds the total losses from power loss state differences. We develop the long timescale LPSS from this approach and express energy saving in the long timescale in terms of the sum of short timescale power saving state differences. Assuming the energy saving over a period T (divided into n very short timescales) is to be estimated for the test scheme relative to the baseline scheme in a scenario comprising m ABSs. Then the energy saving, E_i, in any ABS i is given by:

$$E_i = P_{j_1 k_1} t_1 + P_{j_2 k_2} t_2 + \cdots + P_{j_n k_n} t_n = \sum_r^n P_{j_r k_r} t_r \qquad (25)$$

Where j_r and k_r are the states of the ABS under the baseline and test schemes respectively during the rth timescale, while t_r is the duration of the rth timescale. $P_{j_r k_r}$ is the difference between the power consumption of the baseline state, P_{j_r}, and test state, P_{k_r}, in the rth timescale and thus, it is equivalent to the LPSS state difference of (11). Since, $P_{k_r j_r}$ is also a state difference term, then,

$$P_{j_r k_r} = P_{j_r} - P_{k_r} = -P_{k_r j_r} \qquad (26)$$

$$P_{j_r k_r} = 0 \; ; \; if \; j_r = k_r \qquad (27)$$

From Fig. 3 in section 3.2, there are nine state difference combinations of the three possible states (active (A), idle (I), and sleep (S)) i.e. II, IA, AI, SI, IS, SS, AS, SA, AA. II, SS, and AA lead to zero power saving; IA, SI, and SA lead to power losses; while, AI, IS, and AS lead to power saving. Since from (26) a power loss state difference can be expressed as a negation of a power saving state difference, the energy saving (or loss) can be expressed as a function of the three power saving state differences. Hence

the energy saving (or loss), E_i, of any ABS i can be expressed as:

$$E_i = P_{AI} A_i + P_{IS} B_i + P_{AS} C_i \qquad (28)$$

A_i is summation of timescales associated with AI or IA, B_i is total timescales associated with IS or SI, and C_i is total timescales associated with AS or SA respectively; thus, $A_i, B_i, C_i \in \mathbb{R}$. From (27) the total energy saving (or loss) over all m ABSs, E_{Total}, can be expressed as:

$$\begin{aligned} E_{Total} &= \sum_i^m (P_{AI} A_i + P_{IS} B_i + P_{AS} C_i) \\ &= P_{AI} A_T + P_{IS} B_T + P_{AS} C_T \end{aligned} \qquad (29)$$

$A_T = \sum_i^m A_i$; $B_T = \sum_i^m B_i$; $C_T = \sum_i^m C_i$. Hence, from (29) energy saving over a long timescale will be dependent on how well the test scheme makes decisions that realise the significant positive power saving of LPSS state differences in short timescales during system operation, since some LPSS state differences are almost negligible.

As long timescales may include a large number of short timescales, which might be tedious to analyse in practice, a less cumbersome approach is used which estimates the energy saving based on the total time spent by the ABSs in each state. Assuming the sum of the individual durations spent by the ABSs in the active, idle and sleep states under the baseline scheme are $T_{A,b}$, $T_{I,b}$, and $T_{S,b}$ respectively while $T_{A,t}$, $T_{I,t}$, and $T_{S,t}$ are the equivalent durations for the test scheme; then the total baseline energy consumption, E_b, and the total test scheme energy consumption, E_t, are as follows:

$$E_b = P_A T_{A,b} + P_I T_{I,b} + P_S T_{S,b} \qquad (30)$$

$$E_t = P_A T_{A,t} + P_I T_{I,t} + P_S T_{S,t} \qquad (31)$$

P_A, P_I, P_S are the power consumption of an ABS in the active, idle, and sleep states respectively. Therefore, the total energy saving, E_{Total}, in terms of the duration in the different states is given by:

$$E_{Total} = P_A (T_{A,b} - T_{A,t}) + P_I (T_{I,b} - T_{I,t})$$

$$+ P_S (T_{S,b} - T_{S,t}) \qquad (32)$$

If N_{abs} is the number of ABSs in the network, then the average energy saving per ABS, $\overline{E_{Total}}$ is therefore:

$$\overline{E_{Total}} = P_A \frac{(T_{A,b} - T_{A,t})}{N_{abs}} + P_I \frac{(T_{I,b} - T_{I,t})}{N_{abs}} + P_S \frac{(T_{S,b} - T_{S,t})}{N_{abs}} \qquad (33)$$

If we define $\overline{T_{A,b}}$ and $\overline{T_{A,t}}$ as average duration of an ABS in the active state under the baseline and test schemes respectively, then we can define a difference term that indicates how effective the test scheme is in reducing active duration of ABSs relative to the baseline. We refer to this term as the *net average active duration*, $\overline{T_{A,net}}$, therefore:

$$\overline{T_{A,net}} = \frac{(T_{A,b} - T_{A,t})}{N_{abs}} \tag{34}$$

Similarly, the *net average idle duration,* $\overline{T_{I,net}}$, and *net average sleep duration,* $\overline{T_{S,net}}$, are given by:

$$\overline{T_{I,net}} = \frac{(T_{I,b} - T_{I,t})}{N_{abs}} \tag{35}$$

$$\overline{T_{S,net}} = \frac{(T_{S,b} - T_{S,t})}{N_{abs}} \tag{36}$$

The net average durations of (34), (35), and (36) cannot all be positive since the test scheme will prioritize ABSs operating in some states over the other states.

4. Simulation Results and Discussion

In order to understand how the energy saving and QoS varies across power models on a large scale, the complete separation architecture described in section 2 is modelled in MATLAB. 5 HBSs, 9 ZBSs and 112 ABSs are deployed in the network, while 6,000 MSs are distributed uniformly outdoors along the streets. Monte Carlo simulations are performed to evaluate the energy savings of the test scheme relative to the baseline scheme, (i.e. the highest SINR scheme) under different power model assumptions representing different BS enhancements. The simulation parameters are specified in Table 2. Two cases of the test scheme are compared with the baseline scheme. The first one is implemented without the Topology Management (TM) scheme in order to evaluate the effect of transitions to the idle state only (termed idle state saving) on both QoS and energy saving. The second case involves both the IACCR resource management scheme and the TM scheme and shows the added benefit of sleep state transitions.

In all instances, each user arrives into the system with a fixed file size of 2MB to upload and the arrival rate of users into the system has a Poisson distribution with a mean λ. Admission control is used to determine whether a user data request is served or not. If the uplink SINR achieved by the user exceeds the SINR admission threshold, the user is admitted into the network but if the uplink SINR achieved is lower than the threshold, the user is denied access or blocked. We define the system's acceptable range of operation as the region where the blocking probability is less than 5% and the energy saving is above zero. Blocking probability threshold of 5% or lower has been used previously in the literature (e.g. [56], [57], and [58]) for state of the art LTE network. However, the threshold does not affect the comparison of the different power models rather it shows the relative performance of the resource management strategies in terms of QoS. The simulation results are evaluated over durations required to achieve 100,000 iterations in all cases.

The QoS is measured in terms of blocking probability and average file transfer delay. In this work, admission control is used to determine whether a user data request would be served or not. If the SINR achieved by the user exceeds the admission threshold, the user is admitted into the network but if the SINR achieved is lower than the threshold, the user is denied access or blocked. The blocking probability is measured in terms of the file requests that are blocked by the network. Hence, the blocking probability, P_b, is given by:

$$P_b = \frac{N_B}{N_T} \tag{37}$$

where N_B is the total number of blocked file transmission requests and N_T is the total number of file requests.

The file transfer delay of a successfully transmitted user file is measured as the time between the instance the file transfer request is made and the instance the file is received in its entirety at the receiver. Queuing delay is not considered, once a free resource is available to serve a file request it is processed, otherwise it is blocked and retransmitted at a later time. The file transfer delay of all successfully transmitted files is averaged to obtain the average file transfer delay. Thus the average file transfer delay, $\overline{D}$, is given as:

$$\overline{D} = \frac{D_T}{N} \tag{38}$$

where D_T is the sum of the file transfer delay of all successfully transmitted files and N is total number of successfully transmitted files.

The third choice of ABS is set as the restriction level for MSs in the IACCR scheme. It is important to note that the QoS performance will be the same irrespective of the power model because what has been done is to consider the power that will be consumed for different schemes assuming a certain type of BS generation. The maximum transmission power is the same for all power models considered.

Table 2
Simulation Parameters [42]

Parameter	Value
Deployment area dimension	1350m×1350m
Street width	15 m
Building block size	75m×75m
ABS antenna height	5m
MS antenna height	1.5m
Carrier Frequency	3.5GHz
MS Transmit Power	23dBm
ABS Maximum Gain	17dBi
Noise Floor	-174dBm/Hz
Call Admission SINR	10dB
Minimum SINR for Reception	1.8dB
SINR for highest throughput	21dB

Fig. 9 shows that the baseline scheme, i.e. highest SINR scheme, has the best blocking probability performance. This is because all ABSs are always on and MSs are served by their closest and first choice ABSs. The test scheme without TM, i.e. IACCR without TM, has blocking probability comparable to the highest SINR below medium traffic load (less than 150 files/s).

However, as traffic load increases the interference becomes more and more significant because of the permission of connection to other choices apart from the first choice. Thus, it has much poorer blocking probability with respect to the baseline scheme at high traffic load (above 150 files/s). The blocking probability is further worsened by allowing idle ABSs to be switched off (i.e. IACCR with TM). This is because when ABSs are switched off, options of ABSs available for data services reduce and alternatives are in sleep state when active ABSs have no suitable channel.

The delay performance shown in Fig. 10 follows a similar trend as the blocking probability. Again, the highest SINR scheme has the best performance and this is because MSs use the highest SINR possible for transmission and therefore completes transmission faster. The "IACCR without TM scheme" causes many MSs to operate at lower SINRs than the highest SINR due to permission of second and third choice connections. Thus, higher average file transfer delay is experienced under the test scheme. The delay is further increased when idle ABSs are allowed to sleep. This is because more distant MS to ABS connections will be experienced and even lower SINRs will be utilized than when idle ABSs are not put into sleep state.
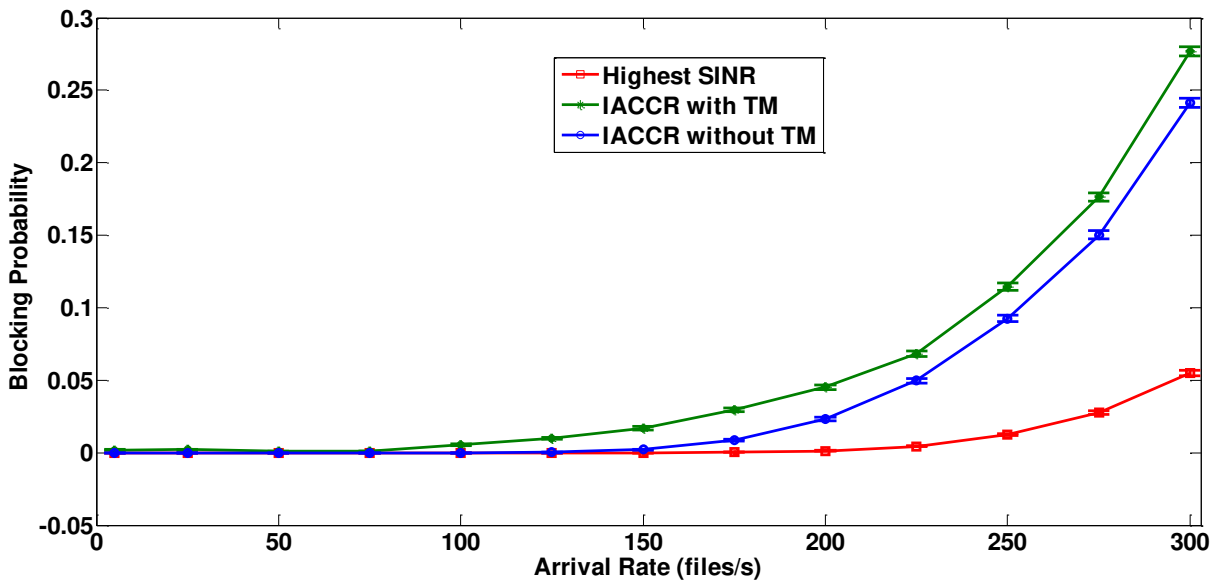

Fig. 9. Blocking probability of baseline scheme and Test scheme without TM and with TM
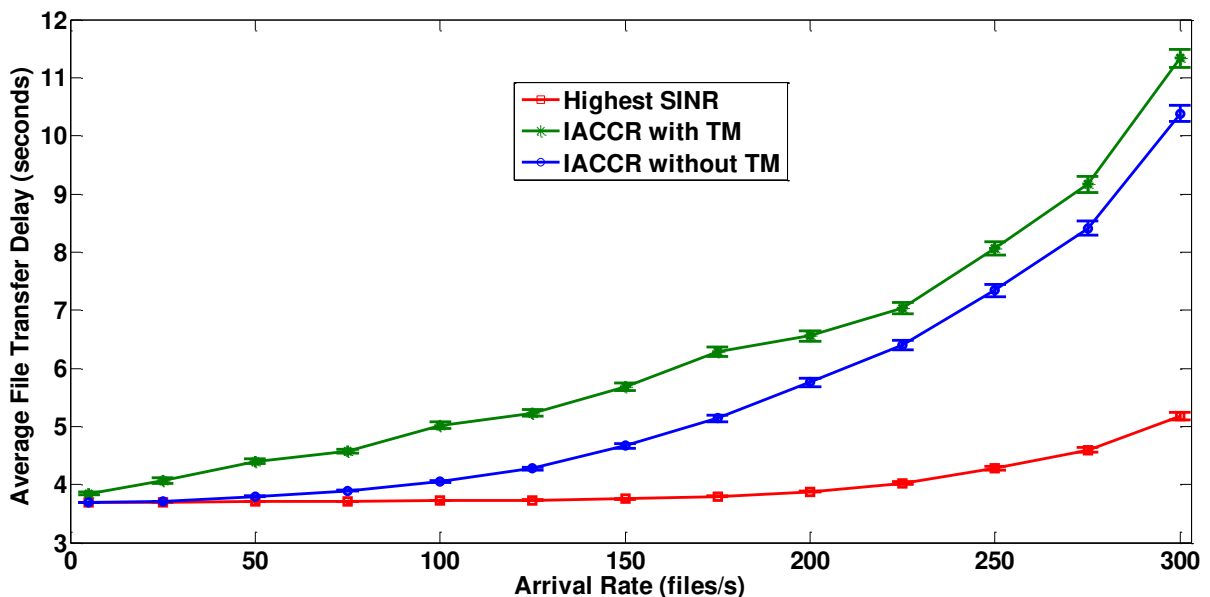

Fig. 10. Average delay of baseline scheme and test scheme without TM and with TM

The net average durations of (34), (35), and (36) are normalized by the duration of observation and expressed as percentages. The net average duration of an ABS when sleep state is not permitted (i.e. without TM) is shown in Fig. 11. It is observed at the lowest traffic load (5 files/s) that the net average duration is nearly zero for both active and idle states. This is because a very small number of ABSs is required simultaneously at such a very low traffic load to serve users and there is hardly any room for benefitting from clustering MSs with few ABSs. However, at higher traffic loads (up to 125 files/s) the highest SINR scheme serves MSs with higher number of ABSs (in active state) relative to the test scheme. The test scheme effectively leaves some of the active ABS under the baseline scheme in idle state. Hence, the net average active duration is increasingly positive while the net average idle duration is increasingly negative. Thus, the state difference in this case is only Active to Idle (AI) and it is a power saving LPSS type. As the traffic load increases further the trend is reversed and eventually both net average durations reach zero at 300 files/s. This is as a result of higher interference at higher loads beyond 125 files/s which makes it increasingly difficult for the test scheme to cluster MSs with few ABSs.

The energy saving for the test scheme without TM is shown in Fig. 12 for the different power models. SotA 2010, Improved DTX and Market 2014 are nearly zero because the LPSS gain for AI is negligible for these power models as explained with the comparative LPSS gain and shown in Fig. 8. However, significant energy saving is achieved with Beyond 2020, Han and Future models, as the LPSS gain for AI is significant for these set of models. The

energy saving trend of these models follows the trend of the net average duration of Fig. 11. It increases as the AI gain increases and decreases when the AI gain decreases. Also, the Future and Han models have higher savings than the Beyond 2020 model. This is because the Future model assumes ABSs have very low idle state consumption like sleep state; while the Han model assumes ABSs have high uplink active consumption. The Beyond 2020 model assumes more moderate idle and active state consumptions, thus the lower saving noticed.

The net average duration of an ABS when sleep state is supported (i.e. with TM) is shown in Fig. 13. It is observed that the net average active duration and the net average idle duration are both positive while the net average sleep duration is negative. Therefore, the state differences in this case are Active to Sleep (AS) and Idle to Sleep (IS) and both state differences are LPSS state differences. The net average active duration (like in the no TM case in Fig. 11) rises from a near zero value at the lowest traffic load to a peak value (at 50 files/s) and then gradually depreciates until it reduces to zero at the highest traffic load. Comparatively, while unused ABSs are left in the idle state in the baseline scheme, in the test scheme these unused ABSs would be put to sleep alongside the active ABSs under the baseline scheme operated in the sleep state under the test scheme for similar time periods. At low loads, the net average idle duration is high but as traffic load increases, the baseline scheme requires more ABSs to be in active state. Thus, the net average idle duration is negligible beyond 100 files/s. As a result below 100 files/s power saving state differences are both AS and IS but mainly AS after 100 files/s.
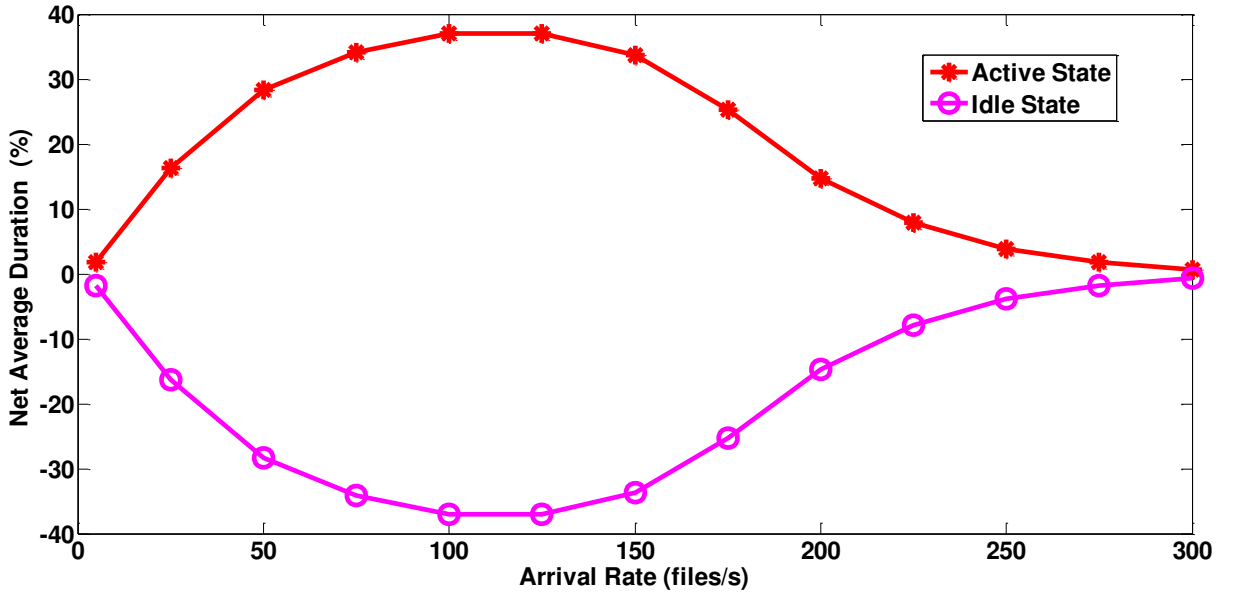

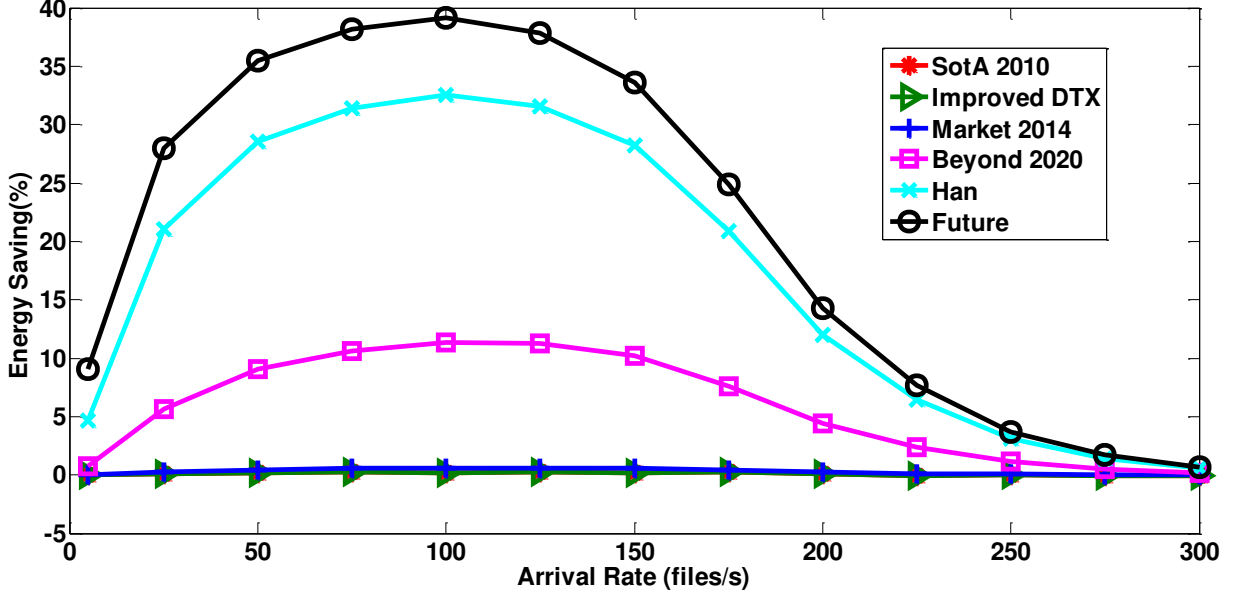**Fig. 11.** Net average duration of ABS for different ABS states when TM is not permitted

Fig. 12. Energy saving of test scheme without TM for different power model assumptions
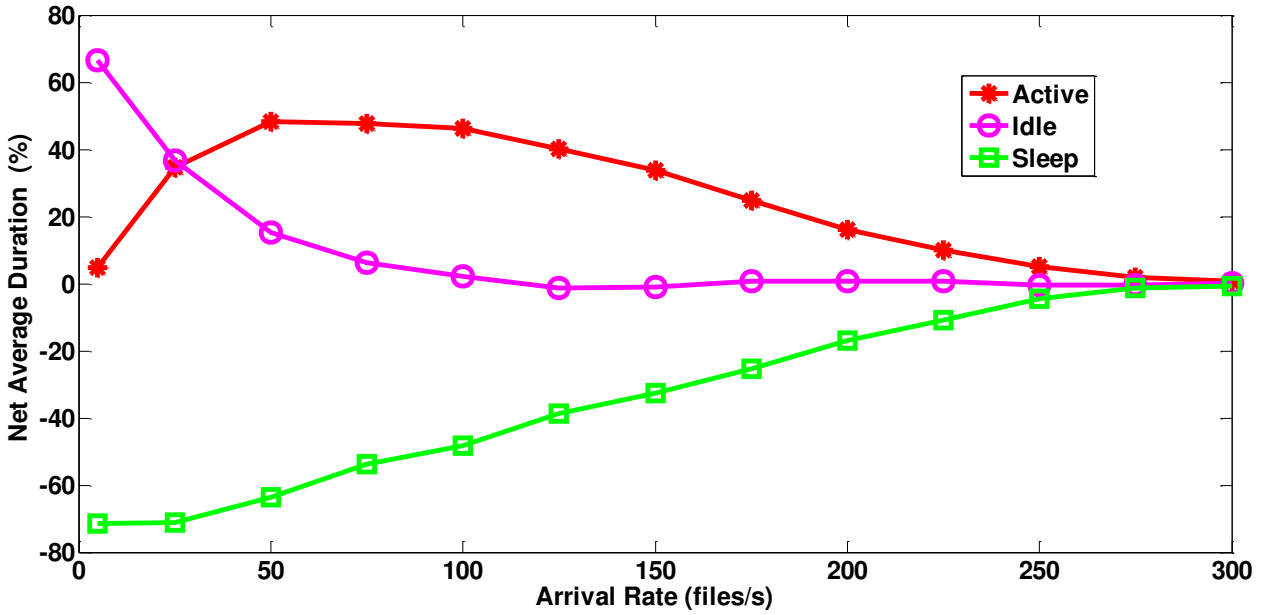

Fig. 13. Net average duration of ABS for different states when TM is permitted

The energy saving for the different power models when TM is applied in the test scheme is shown in Fig. 14. At the lowest load of 5 files/s, as can be observed in Fig. 13, the IS state difference is the predominant power saving state difference because the net average idle duration is significantly higher than the net average active duration. Since the IS state difference gives zero savings for the Future model as shown under the Comparative LPSS of Fig. 8, it has relative low energy saving obtained for the small AS state difference at 5 files/s. However, as the AS state difference duration increases with increasing traffic load, the energy saving increases and reaches its peak when the AS duration also reaches its peak. Beyond 2020 and Han Models benefit from IS state difference but to lower degree compared to the AS state difference (as observed under Comparative LPSS in Fig. 8). Therefore, both models only reach their peak values after the AS state difference becomes significant. The other models (SotA 2010, Improved DTX and Market 2014) benefit nearly equally from both AS and IS state differences and are therefore at peak values at the lowest traffic load. Energy saving reduces to zero at the highest load when there are no state differences.
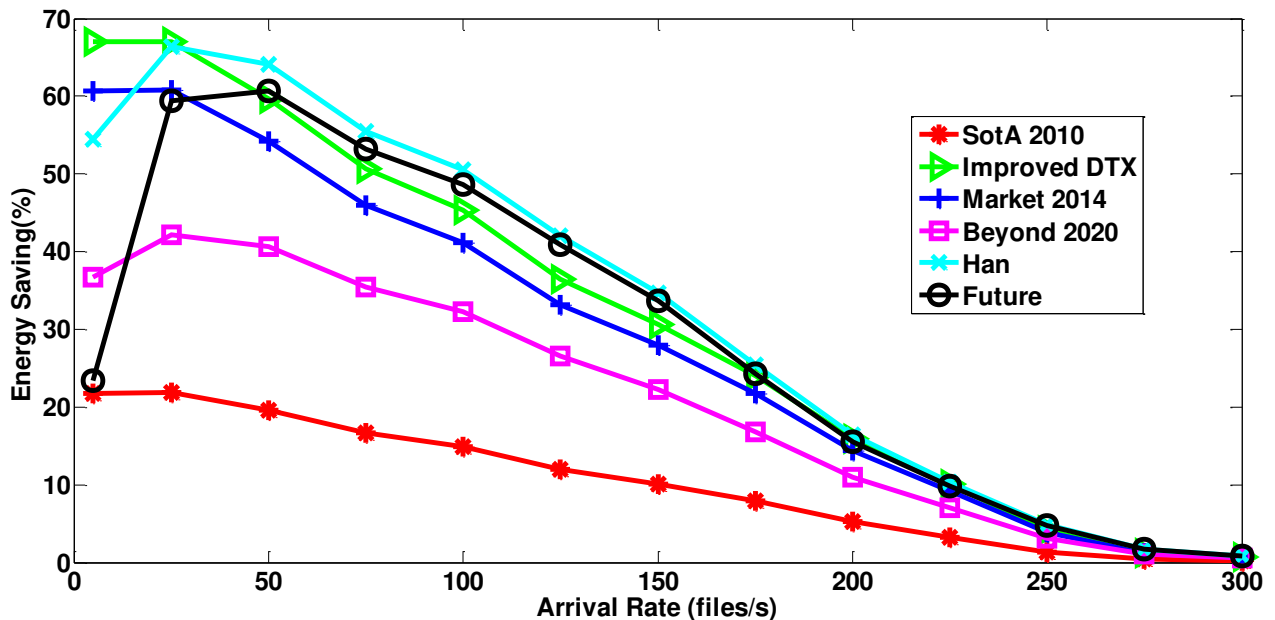
Fig. 14. Energy saving of test scheme with TM for different power model assumptions

The SotA 2010 model achieves the lowest energy saving (up to 21%) because of the high sleep consumption while the massive reduction of sleep state consumption in the Improved DTX and Market 2014 models lead to high energy savings (up to 61% and 67% respectively). Although, the no load consumption is reduced significantly for both Han and Future Models, their energy savings are comparable with the Improved DTX because sleep mode consumption is almost zero in both cases. More conservative sleep mode consumption is assumed for the Beyond 2020 model and the energy saving is lower (up to 42%).

5. Conclusion

In this paper, a framework has been developed to study the impact of power model assumptions on the energy saving achievable by operating small cell BSs in low power states rather than higher power states (referred to as Low Power State Saving (LPSS)) in a 5G separation architecture. We identify BS state changes or state differences that results in LPSS and compute LPSS gain over very short timescales for different power models. It is shown that these short timescale LPSS gains determine energy saving performance in multiple BS scenarios and over long timescales. Simulation results show that energy saving of an energy efficient resource management scheme relative to a baseline, high capacity density focussed scheme varies across different power models as a function of model-specific significant LPSS state differences.

Also, if the separation architecture is based on existing small cell BS modelled by SotA power models, energy saving is totally dependent on sleep mode activation (i.e. AS and IS) for energy savings. Whereas future small cell BSs modelled by more visionary power models can achieve

energy saving through both idle and sleep state BS operation (i.e. AI, AS and IS). Therefore, future small cell BSs can still save energy through idle state operation at high traffic load even if longer BS waiting time before sleep are introduced or sleep state transition is prohibited to improve QoS performance. This insight can be applied to enhance the TM scheme presented in this paper to prohibit or permit sleep mode transitions depending on the traffic load. Such an enhanced TM scheme is being studied for use in the development of an adaptive joint resource and topology management scheme as the future work. Peak energy savings ranging from 21% to 67% are obtained across the power models. More importantly, up to 42% energy saving is obtained for the Beyond 2020 model which is based on less than the ideal assumptions of the Future model.

References

[1] I. Chih-Lin, C. Rowell, H. Shuangfeng, X. Zhikun, L. Gang, and P. Zhengang, "Toward green and soft: a 5G perspective," *IEEE Communications Magazine,* vol. 52, pp. 66-73, 2014.

[2] M. Olsson, C. Cavdar, P. Frenger, S. Tombaz, D. Sabella, and R. Jantti, "5GrEEn: Towards Green 5G mobile networks," in *IEEE Wireless and Mobile Computing, Networking and Communications*, 2013, pp. 212-216.

[3] S. Buzzi, I. C. L, T. E. Klein, H. V. Poor, C. Yang, and A. Zappone, "A Survey of Energy-Efficient

Techniques for 5G Networks and Challenges Ahead," *IEEE Journal on Selected Areas in Communications,* vol. 34, pp. 697-709, 2016.

[4] J. Wu, Y. Zhang, M. Zukerman, and E. K. N. Yung, "Energy-Efficient Base-Stations Sleep-Mode Techniques in Green Cellular Networks: A Survey," *IEEE Communications Surveys & Tutorials,* vol. 17, pp. 803-826, 2015.

[5] M. Ismail, W. Zhuang, E. Serpedin, and K. Qaraqe, "A Survey on Green Mobile Networking: From The Perspectives of Network Operators and Mobile Users," *IEEE Communications Surveys & Tutorials,* vol. 17, pp. 1535-1556, 2015.

[6] T. H. Congzheng Han, Simon Armour, Ioannis Krikidis, "Green radio: radio techniques to enable energy-efficient wireless networks," *IEEE Communications Magazine,* vol. 49, pp. 46 - 54 2011.

[7] J. G. Andrews, S. Buzzi, W. Choi, S. Hanly, A. Lozano, A. C. Soong*, et al.*, "What will 5G be?," *IEEE Journal on Selected Areas in Communications,* vol. 32, pp. 1065-1082, 2014.

[8] F. Haider, X. Gao, X.-H. You, Y. Yang, D. Yuan, H. M. Aggoune*, et al.*, "Cellular architecture and key technologies for 5G wireless communication networks," *IEEE Communications Magazine,* p. 123, 2014.

[9] A. Zappone, L. Sanguinetti, G. Bacci, E. Jorswieck, and M. Debbah, "Energy-Efficient Power Control: A Look at 5G Wireless Technologies," *IEEE Transactions on Signal Processing,* vol. 64, pp. 1668-1683, 2016.

[10] F. Boccardi, R. W. Heath, A. Lozano, T. L. Marzetta, and P. Popovski, "Five disruptive technology directions for 5G," *IEEE Communications Magazine,* vol. 52, pp. 74-80, 2014.

[11] X. Xu, G. He, S. Zhang, Y. Chen, and S. Xu, "On functionality separation for green mobile networks: concept study over LTE," *IEEE Communications Magazine,* vol. 51, pp. 82-90, 2013.

[12] A. Capone, I. Filippini, B. Gloss, and U. Barth, "Rethinking cellular system architecture for breaking current energy efficiency limits," in *Sustainable Internet and ICT for Sustainability (SustainIT),* pp. 1-5, 2012

[13] T. Zhao, P. Yang, H. Pan, R. Deng, S. Zhou, and Z. Niu, "Software defined radio implementation of signaling splitting in hyper-cellular network," in *Proceedings of the second workshop on Software radio implementation forum*, pp. 81-84, 2013.

[14] S. Mukherjee and H. Ishii, "Energy efficiency in the phantom cell enhanced local area architecture," in *IEEE Wireless Communications and Networking Conference*, pp. 1267-1272, 2013.

[15] Z. Wang and W. Zhang, "A Separation Architecture for Achieving Energy-Efficient Cellular Networking," *IEEE Transactions on Wireless Communications, ,* vol. 13, pp. 3113-3123, 2014.

[16] X. Zhang, J. Zhang, W. Wang, Y. Zhang, Z. Pan, G. Li*, et al.*, "Macro-assisted data-only carrier for 5G green cellular systems," *IEEE Communications Magazine,* vol. 53, pp. 223-231, 2015.

[17] Z. Chen, L. Qiu, and X. Liang, "Energy-Efficient Combination of Small Cells and Multi-Antenna Under Separation Architecture," *IEEE Communications Letters,* vol. 19, pp. 1572-1575, 2015.

[18] J. Wu, S. Zhou, Z. Niu, C. Liu, P. Yang, and G. Miao, "Traffic-aware data and signaling resource management for green cellular networks," in *IEEE International Conference on Communications,* pp. 3499-3504, *2014.*

[19] Z. Shan, W. Jian, G. Jie, Z. Sheng, and N. Zhisheng, "Energy-optimal probabilistic base station sleeping under a separation network architecture," in *IEEE Global Communications Conference,* pp. 4239-4244, 2014.

[20] Z. Zhisheng, X. Guo, S. Zhou, and P. R. Kumar, "Characterizing Energy-Delay Tradeoff in Hyper-Cellular Networks with Base Station Sleeping Control," *IEEE Journal on Selected Areas in Communications, ,* vol. 33, pp. 641-650, 2015.

[21] Z. Shan, G. Jie, Z. Sheng, and N. Zhisheng, "How Many Small Cells Can be Turned Off via Vertical Offloading Under a Separation Architecture?," *IEEE Transactions on Wireless Communications,* vol. 14, pp. 5440-5453, 2015.

[22] E. Ternon, P. K. Agyapong, and A. Dekorsy, "Performance evaluation of macro-assisted small cell energy savings schemes," *EURASIP Journal on Wireless Communications and Networking,* vol. 2015, pp. 1-23, 2015.

[23] A. M. Abdelhady, O. Amin, and M. S. Alouini, "Resource allocation for phantom cellular networks: Energy efficiency vs spectral efficiency," in *IEEE International Conference on Communications*, pp. 1-6, 2016.

[24] S. Zhang, N. Zhang, S. Zhou, J. Gong, Z. Niu, and X. Shen, "Energy-Aware Traffic Offloading for Green Heterogeneous Networks," *IEEE Journal on Selected Areas in Communications,* vol. 34, pp. 1116-1129, 2016.

[25] J. Zhang, X. Zhang, and W. Wang, "Cache-Enabled Software Defined Heterogeneous Networks for Green and Flexible 5G Networks," *IEEE Access,* vol. 4, pp. 3591-3604, 2016.

[26] Y. Chen, X. Wen, Z. Lu, H. Shao, and W. Jing, "Cooperation-enabled energy efficient base station management for dense small cell networks," *Wireless Networks,* pp. 1-18, 2016.

[27] X. Guo, Z. Niu, S. Zhou, and P. R. Kumar, "Delay-Constrained Energy-Optimal Base Station Sleeping Control," *IEEE Journal on Selected Areas in Communications,* vol. 34, pp. 1073-1085, 2016.

[28] G. Lee and H. Kim, "Green Small Cell Operation of Ultra-Dense Networks Using Device Assistance," *Energies,* vol. 9, p. 1065, 2016.

[29] J. Yang, X. Zhang, and W. Wang, "Two-stage base station sleeping scheme for green cellular networks," *Journal of Communications and Networks,* vol. 18, pp. 600-609, 2016.

[30] 3GPP, "TR 36.842: "Study on Small Cell Enhancements for E-UTRA and E-UTRAN; Higher layer aspects" version 12.0.0 Release 12," 2013.

[31] A. Prasad and A. Maeder, "Backhaul-aware energy efficient heterogeneous networks with dual connectivity," *Telecommunication Systems,* vol. 59, pp. 25-41, 2015.

[32] Y. Wu, K. Guo, J. Huang, and X. S. Shen, "Secrecy-Based Energy-Efficient Data Offloading via Dual Connectivity Over Unlicensed Spectrums," *IEEE Journal on Selected Areas in Communications,* vol. 34, pp. 3252-3270, 2016.

[33] G. Auer, V. Giannini, I. Godor, P. Skillermark, M. Olsson, M. A. Imran*, et al.*, "Cellular Energy Efficiency Evaluation Framework," in *IEEE Vehicular Technology Conference*, pp. 1-6, 2011.

[34] G. Auer, V. Giannini, C. Desset, I. Godor, P. Skillermark, M. Olsson*, et al.*, "How much energy is needed to run a wireless network?," *IEEE Wireless Communications,* vol. 18, pp. 40-49, 2011.

[35] P. Frenger, P. Moberg, J. Malmodin, Y. Jading, and I. Godor, "Reducing Energy Consumption in LTE with Cell DTX," in *IEEE Vehicular Technology Conference*, pp. 1-5, 2011.

[36] L. M. Correia, D. Zeller, O. Blume, D. Ferling, Y. Jading, Go*, et al.*, "Challenges and enabling technologies for energy aware mobile radio networks," *IEEE Communications Magazine,* vol. 48, pp. 66-72, 2010.

[37] H. Holtkamp, G. Auer, and H. Haas, "On Minimizing Base Station Power Consumption," in *IEEE Vehicular Technology Conference,* pp. 1-5, 2011.

[38] B. Debaillie, C. Desset, and F. Louagie, "A flexible and future-proof power model for cellular base stations," in *IEEE Vehicular Technology Conference,* pp. 1-7, 2015.

[39] O. Marinchenko, C. Naftali, M. Goldhamer, A. Burr, A. Papadogiannis, M. Dohler*, et al.*, "BuNGee project overview," in *IEEE International Conference on Microwaves, Communications, Antennas and Electronic Systems (COMCAS 2011)*, 2011.

[40] M. Goldhamer, Z. Gross, N. Haklai, N. Lavi, O. Marinchenco, P. Michalski*, et al.*, "BuNGee Deliverable D1.2: Baseline BuNGee Architecture," http://www.ict-bungee.eu, accessed April, 2013.

[41] M. H. Noy Blum, Rami Dagan, Vered Tsukerman, Ilan Matitiahu, Ziv Dashevsky, Shmuel Hager, Oleg Marinchenco, Nikolaos Bartzoudis, "BuNGee Deliverable: D4.4 BuNGee Live Test Evaluation Report," , http://www.ict-bungee.eu, accessed April, 2013.

[42] T. Jiang, A. Papadogiannis, D. Grace, and A. Burr, "BuNGee Deliverable: D4.1.1 Interim Simulation " http://www.ict-bungee.eu, accessed April, 2013.

[43] A. Mohamed, O. Onireti, Y. Qi, A. Imran, M. Imran, and R. Tafazolli, "Physical Layer Frame in Signalling-Data Separation Architecture: Overhead and Performance Evaluation," in *Proceedings of European Wireless Conferenc*, pp. 1-6, 2014.

[44] P. Kyosti, Juha Meinilä, Lassi Hentilä, Xiongwen Zhao, Tommi Jämsä, Christian Schneider*, et al.*, "IST-4-027756 WINNER II D1.1.2. WINNER II channel models," http://www.ist-winner.org/WINNER2-Deliverables/D1.1.2v1.1.pdf, 2007.

[45] 3GPP, "TR 36.942: "Evolved Universal Terrestrial Radio Access (EUTRA); Radio Frequency (RF) system scenarios" version 8.2.0 Release 8," ed. http://www.etsi.org/deliver/etsi_tr/136900_136999/136942/08.02.00_60/tr_136942v080200p.pdf, 2009

[46] F. Richter, A. J. Fehske, and G. P. Fettweis, "Energy Efficiency Aspects of Base Station Deployment Strategies for Cellular Networks," in *IEEE Vehicular Technology Conference*, pp. 1-5, 2009.

[47] L. Budzisz, F. Ganji, G. Rizzo, M. A. Marsan, M. Meo, Z. Yi*, et al.*, "Dynamic Resource Provisioning for Energy Efficiency in Wireless Access Networks: A Survey and an Outlook," *IEEE Communications Surveys & Tutorials,* vol. 16, pp. 2259-2285, 2014.

[48] M. Imran and E. Katranaras, "Energy efficiency analysis of the reference systems, areas of improvements and target breakdown. ICT-EARTH Project, Deliverable D2. 3, https://bscw.ict-earth.eu/pub/bscw.cgi/d71252/EARTH_WP2_D2.3_v2.pdf, 2011.

[49] O. Blume, H. Eckhardt, S. Klein, E. Kuehn, and W. M. Wajda, "Energy savings in mobile networks based on adaptation to traffic statistics," *Bell Labs Technical Journal,* vol. 15, pp. 77-94, 2010.

[50] K. Adachi, J. Joung, S. Sun, and P. H. Tan, "Adaptive coordinated napping (conap) for energy saving in wireless networks," *IEEE Transactions on Wireless Communications,* vol. 12, pp. 5656-5667, 2013.

[51] S. Landstrom, H. Murai, and A. Simonsson, "Deployment aspects of LTE pico nodes," in *IEEE International Conference on Communications Workshops,* pp. 1-5, 2011.

[52] H. Yunbo, D. Grace, and P. Mitchell, "Energy efficient topology management for beyond next generation mobile broadband systems," in *International Symposium on Wireless Communication Systems*, pp. 331-335, 2012.

[53] GreenTouch, "GreenTouch Green Meter Research Study: Reducing the Net Energy Consumption in Communications Networks by up to 90% by 2020," http://www.greentouch.org/uploads/documents/Gree

nTouch_Green_Meter_Research_Study_26_June_20
13.pdf, 2013.

[54] A. Fisusi, D. Grace, and P. Mitchell, "Interference aware, energy efficient resource allocation for beyond next generation mobile networks," in *IEEE International Symposium on Personal Indoor and Mobile Radio Communications*, pp. 2197-2202, 2013.

[55] A. Fisusi, D. Grace, and P. Mitchell, "Energy efficient cluster-based resource allocation and topology management for beyond next generation mobile broadband networks," in *IEEE International Conference on Communications Workshops*, pp 576-580, 2013.

[56] N. Morozs, D. Grace, and T. Clarke, "Case-based reinforcement learning for cognitive spectrum assignment in cellular networks with dynamic topologies," in *Military Communications and Information Systems Conference*, pp. 1-6, 2013.

[57] Y.-L. Chung, "Rate-and-power control based energy-saving transmissions in OFDMA-based multicarrier base stations," *IEEE Systems Journal,* vol. 9, pp. 578-584, 2015.

[58] H.-H. Nguyen and W.-J. Hwang, "Energy-Efficient Base Station Operation in Heterogeneous Cellular Networks," *Journal of Korea Multimedia Society,* vol. 15, pp. 1456-1463, 2012.